Parameter Identification for a Slug Test in a Well with Finite-Thickness Skin Using Extended Kalman Filter

By Yen-Chen Huang · Hund-Der Yeh

Abstract Yeh and Chen (J Hydro 342(3–4):283-294, 2007) integrated a slug test solution for a well having a finite-thickness skin with the simulated annealing (SA) to determine the hydraulic parameters of the skin zone and formation zone. Some results obtained in positive-skin scenarios are however not accurate if compared with the target values of the parameters. This study first employs the sensitivity and correlation analyses to quantify the relationship between two normalized sensitivities and analyze the resulting errors in parameter estimates. It is found that the inaccuracy in parameter estimates can be attributed to following two problems: (1) the normalized sensitivities of the skin thickness and hydraulic conductivity are highly correlated and (2) the SA algorithm is very sensitive to round-off error in well-water-level (WWL) data. A parameter identification approach is thus developed based on the extended Kalman filter (EKF) coupled with the solution used by Yeh and Chen (J Hydro 342 (3–4):283-294, 2007) to determine the parameters in six positive-skin scenarios where the parameters were not accurately determined before. We show that previous two problems can be overcome by the proposed approach because it is designed to account for uncertainties of measurements. Moreover, the EKF can save 99.8% and 99.9% computing time when compared with the results using the SA in analyzing 20 WWL data and 47 WWL data, respectively.

1 Introduction

A slug test is performed quickly at a relatively low cost in determining the hydraulic properties of aquifers. The tests involve measuring the recovery of well-water-level (WWL) data in a well after instantaneous injection/withdrawal of a small quantity of water into/from the well. Several mathematical models have been devoted to the analysis of a slug

B. Y.-C. Huang · H.-D. Yeh (✉)
Institute of Environmental Engineering, National Chiao Tung University, Hsinchu 300, Taiwan
e-mail: hdyeh@mail.nctu.edu.tw

test, e.g., Hvorslev (1951), Cooper et al. (1967), Bouwer and Rice (1976), Springer and Gelhar (1991), Hyder et al. (1994), and Butler (1998).

Recently, the wellbore-skin effect has been considered in the analysis of a slug test. A positive skin is defined as a zone adjacent to the wellbore with a hydraulic conductivity smaller than that of the undisturbed formation (Yang and Yeh 2002). In contrast, a negative skin is referred to as a skin zone which has higher hydraulic conductivity than the undisturbed formation. Ramey et al. (1975) proposed an analytical solution for a slug test where the thickness of skin is infinitesimal. The assumption of infinitesimal skin thickness may introduce a large uncertainty because of the similarity in the shape of the type curves. Faust and Mercer (1984) investigated the effect of a finite-thickness skin on the response of slug test by a simple analytical solution and a numerical model. They pointed out that the effect of positive skin leads to an unreliable estimate in aquifer parameters. Following the concept of Faust and Mercer (1984), Moench and Hsieh (1985) presented a Laplace-domain solution with type curves and examined the influences of a finite-thickness skin on the open-well and pressurized slug tests. Yeh and Yang (2006) further extended their Laplace-domain solution to time domain based on the method of Bromwich integral.

Yeh and Chen (2007) combined Moench and Hsieh's solution (1985) with simulated annealing (SA) (Lee et al. 2010; Rani and Moreira 2010) to determine three skin parameters (hydraulic conductivity k_1, specific storage S_{s1}, and skin thickness d_{sk}) and two aquifer parameters (hydraulic conductivity k_2 and specific storage S_{s2}) simultaneously from a slug test performed in a skin-affected confined aquifer system. The skin thickness d_{sk} is equal to r_s-r_w, where r_s and r_w represent the outer radius of the wellbore-skin zone and the effective well radius, respectively. The WWL data were generated by Moench and Hsieh's solution (1985) with a set of standard normally distributed noise added for both positive skin and negative skin scenarios. Some results in the positive skin scenarios showed that the parameters k_2 and d_{sk} were inaccurately determined. They presented a figure of sensitivity analysis to demonstrate that the inaccuracy in these two parameter estimates was caused by insensitivity of aquifer parameters in response to the test and high correlation between the parameters k_1 and d_{sk}. Moreover, the results also indicated that the problem of thin skin thickness causes the inaccuracy in parameter estimation.

Figure 1 shows the normalized sensitivities (Huang and Yeh 2007) of WWL change with respect to the parameter d_{sk} over a 1,000-second interval. There are four curves representing the normalized sensitivities for different values of d_{sk} with given values of the other four parameters (k_1, S_{s1}, k_2, and S_{s2}). The figure indicates that a smaller d_{sk} has a higher normalized sensitivity and quicker response than those of larger d_{sk}. Huang and Yeh (2007) pointed out that the parameters can be accurately estimated once the normalized sensitivity of parameter starts to respond to the change in drawdown. In other words, the aquifer parameters in the case of thin skin thickness should be estimated at least as well as those of thick skin-thickness cases. However, it seems that this finding is not applicable to the case of Yeh and Chen (2007) in which they used SA in searching for the optimal parameter values.

Yeh and Chen (2007, their Table 2) presented the synthetic WWL data generated by Moench and Hsieh's solution (1985). The data, rounded-off to the third decimal, meet the measurement accuracy from engineering viewpoint. However, such inaccuracy in parameter estimation would lead to erroneous results because the algorithm of SA coupled with Moench and Hsieh's solution (1985) is very sensitive to the measurement error in WWL data. In the case of Yeh and Chen (2007, Case 15a in Table 6b, the WWL data without adding noise), the estimated parameters k_1, k_2, S_{s1}, S_{s2}, and d_{sk} based on SA are 2.31×10^{-5} m/s, 9.97×10^{-4} m/s, 1.71×10^{-5} 1/m, 1.83×10^{-5} m/s, and 0.493 m, respectively. However,
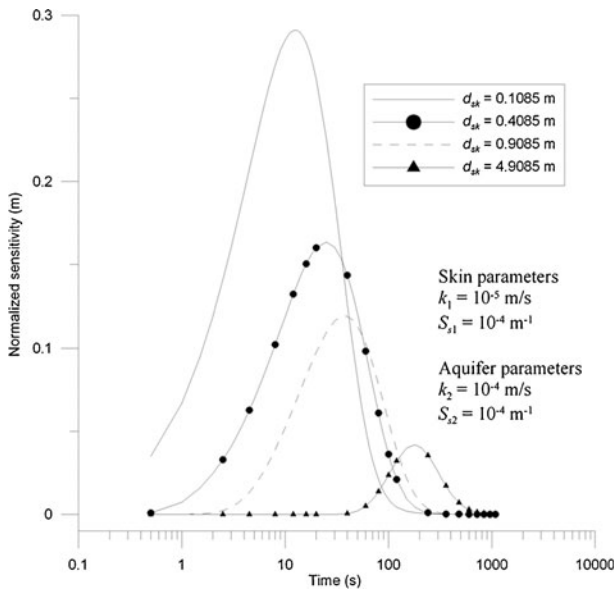
Fig. 1 The normalized sensitivities to the parameter d_{sk} ranged from 0.1085 to 4.9085 m over a time period of 1,000 s

the target parameters are 1.00×10^{-5} m/s, 1.00×10^{-4} m/s, 1.00×10^{-4} 1/m, 1.00×10^{-4} m/s, and 0.1085 m, respectively. The standard error of the estimate (*SEE*) for the predicted WWL is 3.16×10^{-4} m based on the estimated parameters and 3.31×10^{-4} m based on the target parameters.

The *SEE* is defined as $\left(\sum_{j=1}^{n} e_j^2 / v \right)^{\frac{1}{2}}$, where e_j represents the difference between the observed and the predicted WWL and v, the degree of freedom, is equal to the number of observed data points n minus the number of unknowns (Yeh 1987). Such a slightly larger *SEE* value form the target parameters is due to the round-off errors in WWL data. The relative errors (*RE*) of the estimated parameters k_1, k_2, S_{s1}, S_{s2}, and d_{sk} are 131%, −0.3%, −82.9%, −81.7%, and 354%, respectively. Note that the *RE* is defined as the difference between the estimate and target values divided by the target value. This indicates that the SA gives a set of parameters which gives very good fit to the measured WWL data; yet, the estimated parameters are inaccurate in some positive-skin cases.

The problem of inaccuracy in parameter estimation could be improved to some extent by using a longer series of WWL data or analyzing WWL data of the test and observation wells simultaneously (Yeh and Chen 2007). However, the cost and labor spent in the slug test will inevitably increase if more measurements are needed; especially, when extra measurements are taken from observation wells. Moreover, the parameter estimation using SA took about 3.6 h when analyzing a set of 20 WWL data and about 7.6 h for analyzing a set of 47 WWL data when using a personal computer with 3.6 G Pentium IV CPU and 1 GB RAM.

Alternately, the method of extended Kalman filter (EKF) can give accurate parameter estimate because its algorithm accounts for the effects of system and measurement uncertainties in the system measurement model (Grewal and Andrews 1993), and the sequential data assimilation process is more efficient computationally. The Kalman filter was developed by R. E. Kalman in the late 1950s, and its most applications have been in control systems, tracking and navigation of all sorts of vehicles, as well as predictive design of

estimation and control systems. After that, the EKF was proposed for dealing with nonlinear problems (Chou 2011). McLaughlin and Townley (1996) mentioned that the EKF was less likely to converge to an acceptable solution in the parameter estimation problems if the number of unknown parameters was large. They suggested that the EKF may only be able to deal with the case of relative small number of unknown parameters and large amount of the measurements. Drécourt (2003) concluded that the EKF may also be able to determine the parameter if the state and measurement equations were not highly nonlinear. Recently, the EKF was applied to the aquifer parameter and water table related estimations. Leng and Yeh (2003) used EKF and cubic spline to determine the aquifer parameters in both confined and unconfined aquifer systems. Yeh and Huang (2005) employed EKF to determine the aquifer parameters in leaky aquifer systems with and without considering the storage effect in the aquitard. From the analysis of field data, they demonstrated that the EKF can be applied to determine the aquifer parameters successfully. Goegebeur and Pauwels (2007) applied the EKF to a conceptual rainfall-runoff model with 10 parameters and demonstrated its robustness for parameter calibration, especially for problems with high observation errors, infrequent observations, and/or strongly erroneous initial parameters. Shamir et al. (2010) utilized ensemble EKF to link upstream watersheds and channels to main river channels and tributaries in a large regulated basin for flood forecasting. Nenna et al. (2011) applied the EKF approach to invert time-lapse electrical resistivity imaging data collected to observe changes in electrical conductivity under a recharge pond, which is a part of aquifer storage.

In the real-world problems, the skin zone is invisible, immeasurable, and usually very small; thus, the thickness of the skin zone is difficult to accurately determine, especially when the observed data contain measurement errors. Such a challenging task motivates the authors' curiosity to use the EKF. The objective of this study is to investigate and resolve the problem of inaccuracy in the estimation of parameters k_2 and d_{sk} in the positive skin scenarios. The procedure of the analyses to achieve the objective is given below:

1. Using the correlation analysis to quantify the strength of the relationship between the normalized sensitivity of WWL with respect to each of the aquifer parameters over a certain period of time.
2. Utilizing the sensitivity analysis to explore the problem of inaccuracy in the estimation of the parameter k_2.
3. Developing an approach by coupling the EKF with Moench and Hsieh's solution (1985) and analyzing those six positive-skin scenarios in Yeh and Chen (2007) where the parameter k_2 or d_{sk} was not accurately determined.

2 Methodology

This section includes three parts: the first part briefly describes the theory of the EKF, the second part introduce the solution developed by Moench and Hsieh (1985). The third part presents the algorithm of combining EKF with Moench and Hsieh's model (1985) to determinate the hydraulic parameters of the skin and formation zones.

2.1 Discrete Extended Kalman Filter

A nonlinear dynamic system may be expressed as (Grewal and Andrews 1993)

$$x_k = f(x_{k-1}, k-1) + w_k \tag{1}$$

where x_k is a state vector of the system at time step k, $f(x_{k-1}, k-1)$ is a nonlinear function of the system, and w_k is a state noise assumed to be normally distributed with a zero-mean white (uncorrelated) sequence with known covariance Q_k.

The nonlinear implementation equation for the state vector is written as

$$\widehat{x}_k(-) = f(\widehat{x}_{k-1}(+), k-1) \tag{2}$$

where $\widehat{x}_k(-)$ denotes the a priori estimate at k step and $\widehat{x}_k(+)$ represents the *a posteriori* estimate at k-1 step.

Similarly, a measurement model of the system can be written as (Grewal and Andrews 1993)

$$z_k = m(x_k, k) + \upsilon_k \tag{3}$$

where $m(x_k, k)$ is a function for the measurement system and z_k is a measurement vector at time step k. The measurement noise υ_k is assumed to be a white noise with known constant covariance R_k throughout the filtering process.

The nonlinear implementation equation for the measurement is

$$\widehat{z}_k = m(\widehat{x}_k(-), k) \tag{4}$$

where $\widehat{z}_k$ is a predicted measurement vector.

The recursive process of the EKF can be expressed as

$$P_k(-) = E\left[e_k(-)e_k^T(-)\right] = E\left[(x_k - \widehat{x}_k(-))(x_k - \widehat{x}_k(-))^T\right] \tag{5}$$

$$P_k(-) = \Phi_{k-1}P_{k-1}(+)\Phi_{k-1}^T + Q_{k-1} \tag{6}$$

$$\overline{K}_k = P_k(-)M_k^T[M_k P_k(-)M_k^T + R_k]^{-1} \tag{7}$$

$$P_k(+) = \left\{I - \overline{K}_k M_k\right\}P_k(-) \tag{8}$$

$$\widehat{x}_k(+) = \widehat{x}_k(-) + \overline{K}_k(z_k - \widehat{z}_k) \tag{9}$$

where $P_k(-)$ is a priori error covariance matrix, $e_k(-)$ is defined as $x_k - \widehat{x}_k(-)$, Φ_{k-1} is state transition matrix, $\overline{K}_k$ is defined as Kalman gain, $P_k(+)$ is a posteriori covariance, M_k is measurement matrix, and $\widehat{x}_k(+)$ is the updated estimate at step k.

The state transition matrix Φ_{k-1} and measurement matrix M_k can be respectively expressed as

$$\Phi_{k-1} \approx \left.\frac{\partial f(x, k-1)}{\partial x}\right|_{x=\widehat{x}_{k-1}(-)} \tag{10}$$

and

$$M_k \approx \left.\frac{\partial m(x, k)}{\partial x}\right|_{x=\widehat{x}_k(-)} \tag{11}$$

The initial estimates at time step k at some point are required and can be assigned based on the knowledge about the process. With initial estimates and Eqs. (2), (4)–(9), the recursive process of EKF is then established.

The EKF has two advantages over the SA: (1) the EKF can deal with system and measurement uncertainties in the algorithm and (2) the EKF is much more computationally efficient than the SA. The first advantage is that the EKF accounts for the uncertainties in both the system and measurement equations (i.e., w_k in Eq. (1) and υ_k in Eq. (3)). Hence, the impact of uncertainties can be reduced during the determination process if the w_k and υ_k are assigned properly. Contrarily, the SA determines the parameters when searching the optimal results for the objective function in terms of ordinary least squares. The second advantage is that the SA is a "batch" type algorithm that combines all available measurements (WWL in this study) in a single large measurement vector z ($z=[z_1, z_2,\ldots, z_N]^T$, where N is the total number of available measurements). The objective function is then evaluated by calculating entire measurement vector at each step. These evaluations involve huge computing burden, especially when the WWL data set is very long or the model is complicated. Oppositely, the EKF is much efficient since it updates the current estimate using only the newest measurement point at each parameter identification step.

2.2 Moench and Hsieh's Solution (With Considering Skin Effect)

Moench and Hsieh (1985) developed a Laplace domain solution for the response to a drill-stem test in the presence of the skin with finite thickness. Their solution is adequate for the analyses of the open-well slug test in confined aquifers. The schematic diagram of the test is shown in Fig. 2 in which the hydraulic parameters of the skin zone (k_1, S_{s1}, and d_{sk}) are considered. The assumptions leading to the solution are: (1) the aquifer is homogeneous, isotropic, infinite-extent, and of a constant thickness; (2) the well is fully penetrating and with a finite radius; (3) the initial head is constant and uniform throughout the whole aquifer; (4) the
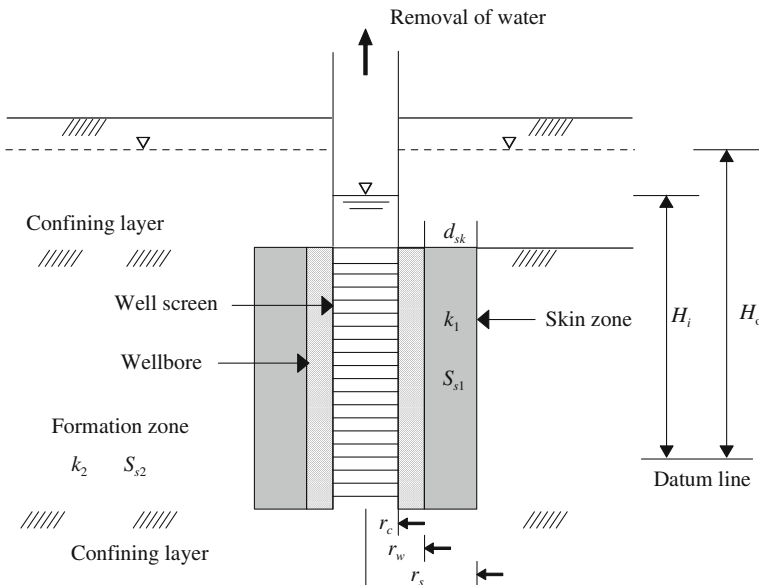

Fig. 2 Schematic diagram of the well and aquifer configurations

vertical flow gradients are negligible; (5) the skin zone is assumed homogeneous and isotropic. The dimensionless form of WWL solution in the Laplace domain can be written as

$$\bar{h} = \frac{\alpha\gamma[\Delta_1 K_0(q\beta) - \Delta_2 I_0(q\beta)]}{c_1\Delta_1 - c_2\Delta_2} \tag{12}$$

with

$$\Delta_1 = \alpha\, I_0(q\beta r_{ds})\, K_1(qr_{ds}) + \beta\, I_1(q\beta r_{ds})\, K_0(qr_{ds}) \tag{13}$$

$$\Delta_2 = \alpha\, K_0(q\beta r_{ds})K_1(qr_{ds}) - \beta\, K_1(q\beta r_{ds})K_0(qr_{ds}) \tag{14}$$

$$c_1 = \alpha\gamma p K_0(q\beta) + \beta q K_1(q\beta) \tag{15}$$

$$c_2 = \alpha\gamma p I_0(q\beta) - \beta q I_1(q\beta) \tag{16}$$

$$\alpha = k_2/k_1 \tag{17}$$

$$\beta = (\alpha S_{s1}/S_{s2})^{1/2} \tag{18}$$

$$\gamma = \frac{\pi r_c^2}{2\pi r_w^2 S_{s2} b} \tag{19}$$

$$r_{ds} = \frac{r_s}{r_w} \tag{20}$$

and

$$q = p^{1/2} \tag{21}$$

where b is aquifer thickness and p is Laplace variable. Moreover, $I_0(.)$ and $I_1(.)$ express the modified Bessel functions of the first kind of order zero and one, respectively; and $K_0(.)$ and $K_1(.)$ are the modified Bessel functions of the second kind of order zero and one, respectively. The inverse Laplace transform of Eq. (12) is calculated by the routine INLAP of IMSL (2003) with the accuracy to five decimal places. This routine, developed based on an algorithm originally proposed by Crump (1976) and later modified by de Hoog et al. (1982), has been successfully applied in some groundwater problems (see, e.g., Chen et al. 1996). The time domain solution for the head $H(t)$ is

$$H(t) = L^{-1}(\bar{h}) \tag{22}$$

where L^{-1} indicates the operator of inverse Laplace transform.

2.3 Application of Proposed Approach in Parameter Identification

The parameters in Eq. (2) at each time step can be expressed as following state vector

$$\widehat{x}_k(-) = [\, k_1 \quad S_{s1} \quad k_2 \quad S_{s2} \quad d_{sk} \,]^T \tag{23}$$

in the proposed approach. For applying to the nonlinear system, the EKF uses the first-order Taylor approximations of state transition and observation equations about the estimated state trajectory. The transition matrix is

$$\Phi_{k-1} \approx \begin{bmatrix}
\frac{\partial k_1}{\partial k_1} & \frac{\partial k_1}{\partial S_{s1}} & \frac{\partial k_1}{\partial k_2} & \frac{\partial k_1}{\partial S_{s2}} & \frac{\partial k_1}{\partial d_{sk}} \\
\frac{\partial S_{s1}}{\partial k_1} & \frac{\partial S_{s1}}{\partial S_{s1}} & \frac{\partial S_{s1}}{\partial k_2} & \frac{\partial S_{s1}}{\partial S_{s2}} & \frac{\partial S_{s1}}{\partial d_{sk}} \\
\frac{\partial k_2}{\partial k_1} & \frac{\partial k_2}{\partial S_{s1}} & \frac{\partial k_2}{\partial k_2} & \frac{\partial k_2}{\partial S_{s2}} & \frac{\partial k_2}{\partial d_{sk}} \\
\frac{\partial S_{s2}}{\partial k_1} & \frac{\partial S_{s2}}{\partial S_{s1}} & \frac{\partial S_{s2}}{\partial k_2} & \frac{\partial S_{s2}}{\partial S_{s2}} & \frac{\partial S_{s2}}{\partial d_{sk}} \\
\frac{\partial d_{sk}}{\partial k_1} & \frac{\partial d_{sk}}{\partial S_{s1}} & \frac{\partial d_{sk}}{\partial k_2} & \frac{\partial d_{sk}}{\partial S_{s2}} & \frac{\partial d_{sk}}{\partial d_{sk}}
\end{bmatrix} \tag{24}$$

This matrix is time invariant, i.e., $\widehat{x}_k = \widehat{x}_{k-1}$. Based on Eq. (6), $P_k(-)$ can be estimated from the known transition matrix Φ_{k-1}. To update the hydraulic parameters in Eq. (7), the Kalman gain $\overline{K}_k$, estimated from the known M_k and the prior covariance matrix $P_k(-)$, is first required. The measurement matrix M_k is the partial derivatives of the estimated drawdown $\widehat{z}_k$. The criterion chosen to terminate the recursive process is expressed as

$$TOL_i = |P_i(k+1) - P_i(k)| \tag{33}$$

where TOL_i is the tolerance for parameter i and $P_i(k)$ is the value of parameter i at time step k. The process will be terminated when all TOL_i meet the values assigned by the users. Figure 3 is a flow chart for the proposed approach in determining parameters when coupled the EKF with Moench and Hsieh's solution (1985). After initializing the estimates of parameters, error covariance matrix P, and the measurement error covariance R, the recursive process starts to compute Eqs. (5)–(9). Note that a set of WWL data is repeatedly used from the beginning once the stepwise determination process of EKF has gone through all data. The estimates of parameters updated based on last measurement point in the data set will be treated as initial estimate for the next run of data assimilation.

3 Results and Discussion

3.1 Correlation and Sensitivity Analyses in Positive Skin Scenarios

The normalized sensitivity of WWL changed with each of five parameters over 1,000 s in a positive skin scenario was demonstrated in Yeh and Chen (2007, Fig. 2b). In this case, the slug test is performed in a homogeneous and isotropic confined aquifer system. The test well fully penetrates the aquifer and the radius of effective well r_w and well casing r_c are 0.0915 m and 0.0508 m, respectively. The sudden drop of WWL is assumed 1 m while the aquifer thickness is 10 m. The WWL data are produced based on Moench and Hsieh's solution (1985). The estimated values of parameters k_1, k_2, S_{s1}, S_{s2}, and d_{sk} are 10^{-5} m/s, 10^{-4} m/s, 10^{-4} m^{-1}, 10^{-4} m^{-1}, and 0.3085 m, respectively. Their figure showed that the normalized sensitivities of parameters k_1, and d_{sk} are symmetrical in shape on the horizontal axis but have different magnitudes, implying that they are highly correlated.
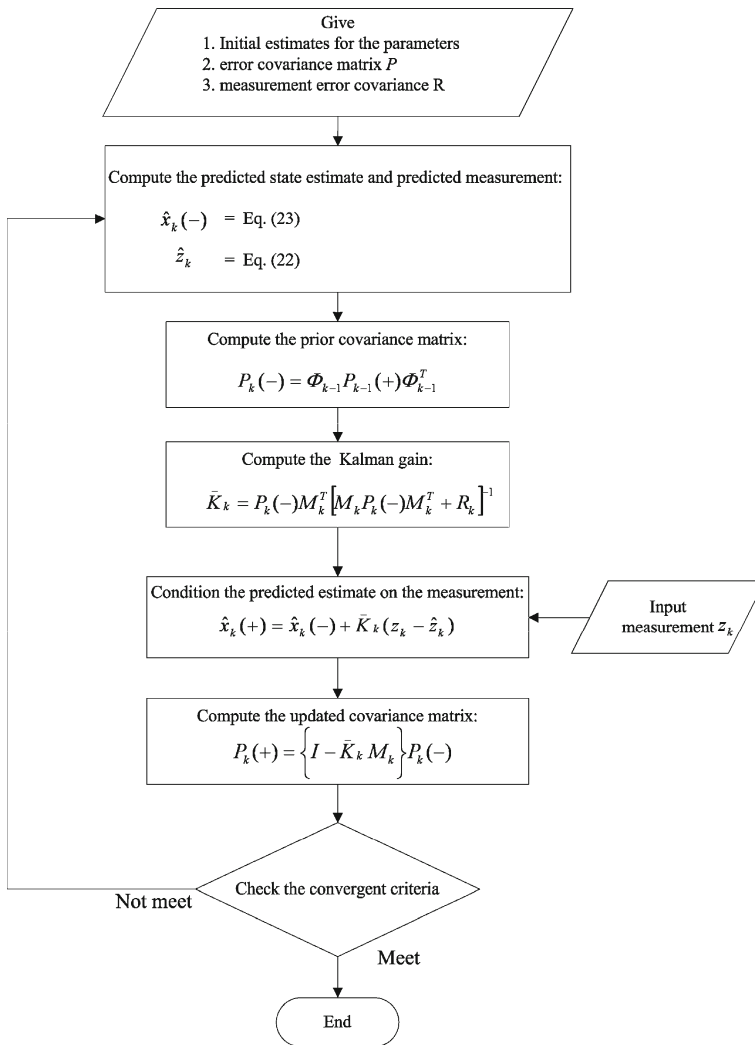
Fig. 3 Flowchart for the EKF for the proposed approach

The correlation analysis is thus used to quantify the strength of the relationship between normalized sensitivities of WWL with respect to each aquifer parameter. The upper and lower parts of Table 1 respectively show the correlation matrices (correlation coefficients for each two variables) of five parameters' normalized sensitivities over 15 and 1,000 s for the same scenario as given in Yeh and Chen (2007, Scenario 2). The bold numbers represent strong correlation between the normalized sensitivities of the parameters. The large value (positive or negative) of the correlation coefficient in these cases signifies that the normalized sensitivities to two parameters vary synchronously over 15 and 1,000 s. In other words, these two parameters begin and stop to influence the WWL almost simultaneously during the test. The upper part of Table 1 displays that the normalized sensitivities of all parameters are highly correlated with each other during first 15-second period. This may reflect that the

Table 1 Two correlation matrices of normalized sensitivities to parameters over periods of 15 and 1,000 s

	15 seconds period				
	k_1	S_{s1}	k_2	S_{s2}	d_{sk}
k_1	1.000	–	–	–	–
S_{s1}	**−0.966**	1.000	–	–	–
k_2	**0.985**	**−0.995**	1.000	–	–
S_{s2}	**0.999**	**−0.979**	**0.993**	1.000	–
d_{sk}	**−1.000**	**0.970**	**−0.987**	**−0.999**	1.000
	1,000 seconds period				
	k_1	S_{s1}	k_2	S_{s2}	d_{sk}
k_1	1.000	–	–	–	–
S_{s1}	0.274	1.000	–	–	–
k_2	**0.896**	−0.093	1.000	–	–
S_{s2}	**0.993**	0.165	**0.935**	1.000	–
d_{sk}	**−0.998**	−0.221	**−0.914**	**−0.998**	1.000

parameters are rather difficult to accurately determine simultaneously using first 15-second data in Yeh and Chen (2007). The lower part of Table 1 shows that the normalized sensitivity to parameter S_{s1} is no longer highly correlated to those of the other parameters during 1,000 s, indicating that S_{s1} behaves differently if compared with those of the other parameters after 15 s.

Yeh and Chen (2007, Table 6a for Scenario 14) indicated that the skin parameters can be determined accurately if the parameters k_1 and k_2 have a distinct difference, i.e., k_2/k_1 is equal to 100. However, the parameter k_2 is still poorly estimated (the relative error RE is 502.06%). Figure 4a and b display the temporal variations of normalized sensitivities to parameters over 1,000 s for the parameter k_1 being equal to 10^{-5} and 10^{-6} m/s, respectively. The values of other parameters are kept the same and given in the figures. In Fig. 4b, the curves of normalized sensitivity to parameters k_2 and S_{s2} are almost invisible. Moreover, the shapes of normalized sensitivities of parameter k_1 and d_{sk} shift to the right as shown in the figure. In other words, the changes of the WWL in response to the relative change of the parameter for k_1 and d_{sk} are slow as compared with those shown in Fig. 4a. Therefore the inaccuracy in parameter k_2 estimation mentioned above may be caused by the problems of small value of k_1 and short WWL data. Obviously, the parameters k_2 and S_{s2} are difficult to accurately determine by analyzing only 15 s WWL data. Figure 5a and b show the normalized sensitivities for the negative skin cases where the values of k_1 are 10^{-4} and 10^{-3} m/s, respectively. The figures depict that the shapes of normalized sensitivity curves do not have significant change even the parameters k_1 and k_2 have distinct values. Hence, the predicted results in negative skin scenarios are more accurate than those of positive skin ones in Yeh and Chen (2007).

3.2 Parameter Determination Using EKF

Six positive skin scenarios in Yeh and Chen (2007, Scenarios 17, 1, 2, 15, 10, and 14) with the RE of estimated k_2 or d_{sk} larger than 100% are selected for testing the applicability of the
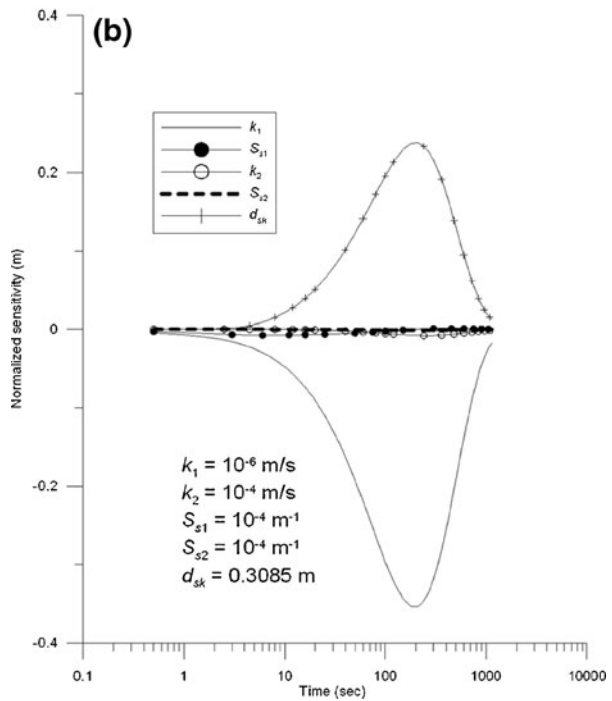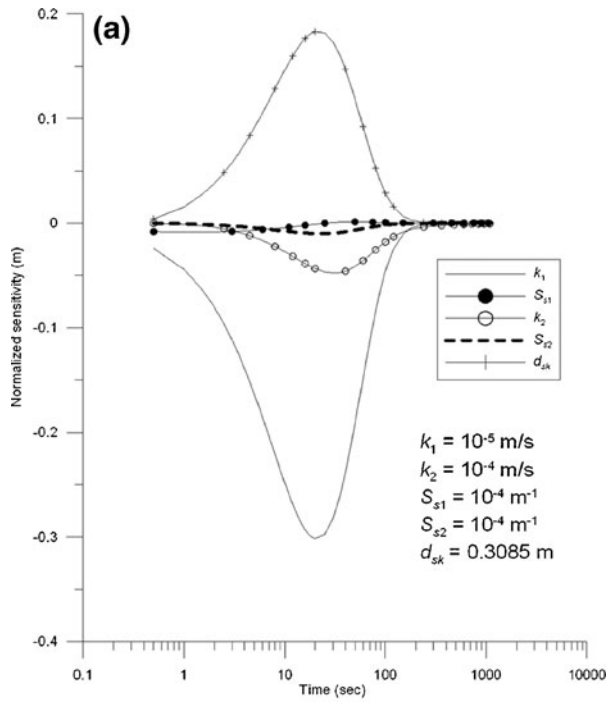
Fig. 5 The normalized sensitivities to five parameters for a negative skin case with $k_2=10^{-5}$ m/s, $S_{s1}=10^{-4}$ m^{-1}, $S_{s2}=10^{-4}$ m^{-1}, $d_{sk}=$ 0.3085 m, and (a) $k_1=10^{-4}$ m/s (b) $k_1=10^{-3}$ m/s

Table 2 The target values and predicted results by analyzing the WWL data within 15 sec and d_{sk} equals 1.3085 (Yeh and Chen 2007, Scenario 17)

Case	Estimated Results				
	k_1 (m/s)	k_2 (m/s)	S_{s1} (1/m)	S_{s2} (1/m)	d_{sk} (m)
Target value	1.00×10^{-5}	1.00×10^{-4}	1.00×10^{-4}	1.00×10^{-4}	1.3085
	Simulated Annealing				
17a	1.01×10^{-5}	2.40×10^{-4}	9.69×10^{-5}	3.19×10^{-5}	1.402
17b	9.95×10^{-6}	1.08×10^{-4}	9.99×10^{-5}	4.30×10^{-5}	1.241
17c	1.00×10^{-5}	9.02×10^{-4}	9.99×10^{-5}	2.33×10^{-5}	1.463
17d	1.02×10^{-5}	7.88×10^{-5}	9.37×10^{-5}	8.36×10^{-5}	1.348
17e	1.00×10^{-5}	5.12×10^{-4}	9.97×10^{-5}	8.75×10^{-5}	1.401
Mean	1.01×10^{-5}	3.68×10^{-4}	9.80×10^{-5}	5.39×10^{-5}	1.371
RE	0.50%	**268.16%**	−1.98%	−46.14%	4.78%
	Extended Kalman Filter				
17a	9.96×10^{-6}	1.50×10^{-4}	1.28×10^{-4}	1.09×10^{-4}	1.343
17b	9.94×10^{-6}	1.47×10^{-4}	1.00×10^{-4}	1.50×10^{-4}	1.321
17c	9.79×10^{-6}	9.76×10^{-5}	1.09×10^{-4}	1.59×10^{-4}	1.311
17d	1.02×10^{-5}	1.45×10^{-4}	9.22×10^{-5}	1.49×10^{-4}	1.460
17e	1.01×10^{-5}	1.52×10^{-4}	9.83×10^{-5}	1.51×10^{-4}	1.373
Mean	1.00×10^{-5}	1.38×10^{-4}	1.06×10^{-5}	1.44×10^{-4}	1.362
RE	−0.03%	38.35%	5.51%	43.65%	4.05%

EKF approach. The *RE* is an appropriate index for error analyses in these hypothetic cases because the target values of the parameters are known a priori. Tables 2, 3, 4, 5, 6 and 7 display the target values and predicted results in those scenarios analyzed by both SA and EKF. All WWL data sets (cases "a" to "e") in these scenarios are the same as those of Yeh and Chen (2007). The cases "b" to "e" in the scenarios represent that four sets of standard normally distributed noise are added to the original WWL data.

Tables 2, 3, 4 and 5 display the predicted results of the five parameters for four positive-skin scenarios (Yeh and Chen 2007, Scenarios 17, 1, 2, and 15) when analyzing 15-second WWL data. The target values of d_{sk} in the scenarios shown in Tables 2, 3, 4 and 5 are 1.3085, 0.9085, 0.3085, and 0.1085 m, respectively. The target values of parameters k_1, k_2, S_{s1}, and S_{s2} are 1.00×10^{-5} m/s, 1.00×10^{-4} m/s, 1.00×10^{-4} m^{-1} and 1.00×10^{-4} m^{-1}, respectively. In Tables 2, 3, 4 and 5, the initial estimates of parameters k_1, k_2, S_{s1}, and S_{s2} for the EKF are 1.5×10^{-5} m/s, 1.5×10^{-4} m/s, 1.5×10^{-4} m^{-1}, and 1.5×10^{-4} m^{-1}. The initial estimates of d_{sk} are 1.4085 m, 1.4085 m, 0.4085 m, and 0.4085 m for the cases of Tables 2, 3, 4 and 5, respectively. The TOL_i for parameters k_1, k_2, S_{s1}, S_{s2}, and d_{sk} are set as 10^{-9} (m/s), 10^{-8} (m/s), 10^{-8} (1/m), 10^{-8} (1/m), and 10^{-5} (m), respectively. In practice, reasonable initial estimates of parameters can generally be made based on the field geology and engineering experiences. Moreover, one can monitor the change of the parameters during the process on-line. Once the parameter values become negative or deviate far from reasonable ranges, the EKF process can be terminated and then restarted with a new set of initial estimates of parameters.
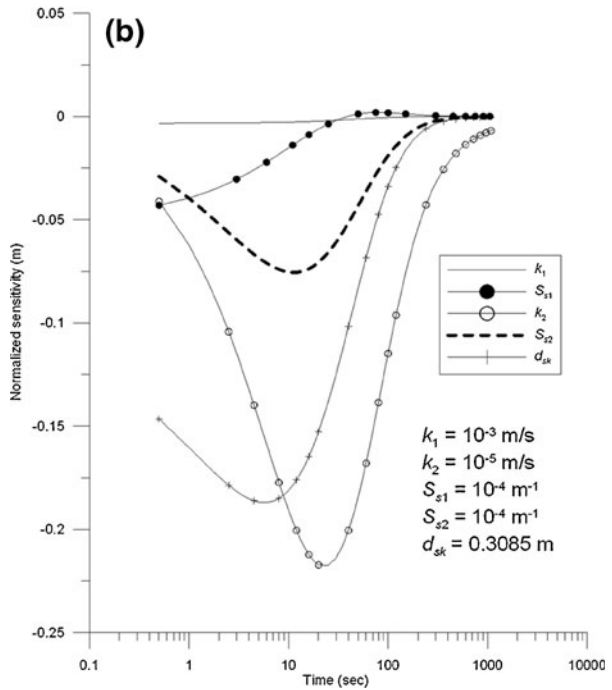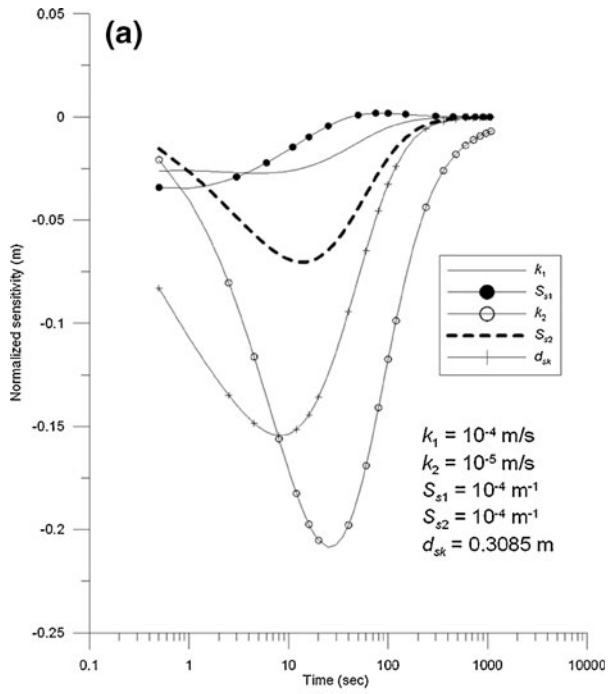
Table 3 The target values and predicted results by analyzing the WWL data within 15 s and d_{sk} equals 0.9085 (Yeh and Chen 2007, Scenario 1)

Case	Estimated Results				
	k_1 (m/s)	k_2 (m/s)	S_{s1} (1/m)	S_{s2} (1/m)	d_{sk} (m)
Target value	1.00×10^{-5}	1.00×10^{-4}	1.00×10^{-4}	1.00×10^{-4}	0.9085
	Simulated Annealing				
1a	1.00×10^{-5}	1.14×10^{-4}	9.94×10^{-5}	4.63×10^{-5}	0.895
1b	1.03×10^{-5}	2.80×10^{-4}	8.98×10^{-5}	2.03×10^{-5}	1.051
1c	1.07×10^{-5}	5.02×10^{-4}	8.17×10^{-5}	7.82×10^{-5}	1.267
1d	1.04×10^{-5}	1.20×10^{-4}	8.76×10^{-5}	8.07×10^{-5}	1.024
1e	1.02×10^{-5}	1.45×10^{-4}	9.51×10^{-5}	5.32×10^{-5}	0.973
Mean	1.03×10^{-5}	2.32×10^{-4}	9.07×10^{-5}	5.57×10^{-5}	1.042
RE	3.20%	**132.20%**	−9.28%	−44.26%	14.69%
	Extended Kalman Filter				
1a	1.01×10^{-5}	1.27×10^{-4}	9.68×10^{-5}	1.51×10^{-4}	0.982
1b	1.01×10^{-5}	1.22×10^{-4}	9.75×10^{-5}	1.46×10^{-4}	0.958
1c	9.99×10^{-6}	1.26×10^{-4}	1.03×10^{-4}	1.23×10^{-4}	0.951
1d	1.01×10^{-5}	9.47×10^{-5}	9.61×10^{-5}	1.35×10^{-4}	0.942
1e	1.03×10^{-5}	1.63×10^{-4}	9.26×10^{-5}	1.57×10^{-4}	1.045
Mean	1.01×10^{-5}	1.26×10^{-4}	9.72×10^{-5}	1.42×10^{-4}	0.976
RE	1.17%	26.37%	−2.77%	42.46%	7.38%

In Table 2, the results of SA show that the parameters k_1 and d_{sk} are determined accurately but k_2 is determined inaccurately. The predicted results of EKF indicate that the parameters k_1, k_2, S_{s1}, and d_{sk} are all determined properly. However, there is slight inaccuracy in parameter S_{s2} estimate with a mean value of 1.38×10^{-4} m^{-1} and RE of 43.65%. Compared with the results of SA, the EKF provides more accurate estimates for all parameters, especially for the parameter k_2. The predicted values of parameter S_{s2} by the EKF are close to the initial estimate. Those results are attributed to the fact that the response of the WWL is generally less sensitivity to S_{s2} than to other parameters. Thus the predicted S_{s2} almost keeps the same value as the initial estimate during the EKF determination processes. In Table 3, the REs of predicted k_1, k_2, S_{s1} and d_{sk} are 1.17%, 26.37%, −2.77% and 7.38%, respectively. Similar to Table 2, the mean value of 1.42×10^{-4} m^{-1} and RE of −42.46% for the parameter S_{s2} show a little inaccurate estimation. In Table 4, the mean values of predicted parameters k_1 and d_{sk} using SA are significantly larger than the target values. Table 1 shows that the normalized sensitivity of parameters k_1 and d_{sk} is significant negatively correlated. An increase in k_1 will reduce the values of WWL; oppositely, an increase in d_{sk} will raise the values of WWL. Therefore, SA may provide a set either highly over-estimated or under-estimated value of the product of these two parameters which can give a very good prediction in WWL data. However, in this scenario, the results of EKF show that all parameters are accurately determined except for the parameter S_{s2}. The REs of parameters k_1, k_2, S_{s1}, S_{s2}, and d_{sk} are are −1.6%, 15.3%, 12.52%, 44.79%, and 1.53%, respectively. In Table 5, the SA results are not accurate for the

Table 4 The target values and predicted results by analyzing the WWL data within 15 s and d_{sk} equals 0.3085 (Yeh and Chen 2007, Scenario 2)

Case	Estimated Results				
	k_1 (m/s)	k_2 (m/s)	S_{s1} (1/m)	S_{s2} (1/m)	d_{sk} (m)
Target value	1.00×10^{-5}	1.00×10^{-4}	1.00×10^{-4}	1.00×10^{-4}	0.3085
	Simulated Annealing				
2a	1.53×10^{-5}	8.50×10^{-5}	3.18×10^{-5}	9.10×10^{-5}	0.856
2b	1.82×10^{-5}	1.08×10^{-4}	1.68×10^{-5}	3.48×10^{-5}	1.486
2c	1.55×10^{-5}	8.09×10^{-5}	3.15×10^{-5}	9.97×10^{-5}	0.907
2d	1.51×10^{-5}	1.07×10^{-4}	3.17×10^{-5}	5.36×10^{-6}	0.683
2e	1.58×10^{-5}	1.08×10^{-4}	2.92×10^{-5}	1.78×10^{-5}	0.869
Mean	1.60×10^{-5}	9.78×10^{-5}	2.82×10^{-5}	4.97×10^{-5}	0.960
RE	59.80%	−2.22%	−71.80%	−50.27%	**211.25%**
	Extended Kalman Filter				
2a	1.02×10^{-5}	1.12×10^{-4}	1.02×10^{-4}	1.51×10^{-4}	0.337
2b	9.17×10^{-6}	1.49×10^{-4}	1.38×10^{-4}	1.77×10^{-4}	0.289
2c	9.80×10^{-6}	1.18×10^{-4}	1.21×10^{-4}	1.46×10^{-4}	0.316
2d	9.79×10^{-6}	1.08×10^{-4}	1.08×10^{-4}	9.34×10^{-5}	0.299
2e	1.03×10^{-5}	8.97×10^{-5}	9.36×10^{-5}	1.56×10^{-4}	0.326
Mean	9.84×10^{-6}	1.15×10^{-4}	1.13×10^{-4}	1.45×10^{-4}	0.313
RE	−1.60%	15.30%	12.52%	44.79%	1.53%

parameters k_1 and d_{sk} estimates. The REs of these two parameters are 157.00% and 601.75%, respectively. However, EKF gives more accurate estimates in k_1 and d_{sk}. Tables 2, 3, 4 and 5 show that the EKF can accurately determine the parameters even in small d_{sk} scenarios. In addition, the EKF can provide consistent estimates of parameters in five cases for each scenario. This behavior demonstrates that the EKF can reduce the uncertainties of measurements significantly.

Table 6 shows the predicted results by both SA and EKF for the same scenario listed in Table 4 but the measurement period of WWL data is extended to 180 s. The initial estimates and the TOL_i of the parameters for the EKF are the same as those of Table 4. The results of SA show a little improvement for d_{sk}, but the RE is still larger than 100%. The results of EKF are as good as those given in Table 4. The REs are −1.75%, 6.22%, 19.59%, 61.25%, and 1.53%, respectively. Table 7 shows the results for a positive skin scenario with largely different hydraulic conductivities between the skin zone and formation zone. The target values are the same as Table 4 except that $k_1 = 10^{-6}$ m/s and the initial estimate of k_1 for the EKF is adjusted to 1.50×10^{-6} m/s. In this case, the results of k_1, S_{s1}, and d_{sk} are improved by using SA but the RE of k_2 is 502.06% which is inaccurately determined. In contrast, the results of EKF display that the parameters k_1, S_{s1}, and d_{sk} determined properly but the parameters k_2 and S_{s2} are slightly inaccurate. The REs of parameters k_1, k_2, S_{s1}, S_{s2}, and d_{sk} are −0.13%, 50.88%, 1.46%, 50.12%, and 1.25%, respectively. The relatively inaccurate estimates of k_2 and S_{s2} are caused by the problem of small value of k_1 where the effect of aquifer properties can not reached to the WWL data within a short period.

Table 5 The target values and predicted results by analyzing the WWL data within 15 s and d_{sk} equals 0.1085 (Yeh and Chen 2007, Scenario 15)

Case	Estimated Results				
	k_1 (m/s)	k_2 (m/s)	S_{s1} (1/m)	S_{s2} (1/m)	d_{sk} (m)
Target value	1.00×10^{-5}	1.00×10^{-4}	1.00×10^{-4}	1.00×10^{-4}	0.1085
	Simulated Annealing				
15a	2.31×10^{-5}	9.97×10^{-5}	1.71×10^{-5}	1.83×10^{-5}	0.493
15b	3.16×10^{-5}	1.05×10^{-4}	7.25×10^{-6}	8.91×10^{-6}	1.324
15c	2.47×10^{-5}	9.34×10^{-5}	1.55×10^{-5}	2.82×10^{-5}	0.629
15d	2.99×10^{-5}	9.97×10^{-5}	6.71×10^{-6}	9.38×10^{-6}	1.015
15a	1.92×10^{-5}	9.66×10^{-5}	2.93×10^{-5}	5.02×10^{-5}	0.346
Mean	2.57×10^{-5}	9.89×10^{-5}	1.52×10^{-5}	2.30×10^{-5}	0.761
RE	**157.00%**	−1.12%	−84.83%	−77.00%	**601.75%**
	Extended Kalman Filter				
15a	9.88×10^{-6}	9.63×10^{-5}	1.28×10^{-4}	1.09×10^{-4}	0.109
15b	1.04×10^{-5}	1.06×10^{-4}	1.50×10^{-4}	1.25×10^{-4}	0.106
15c	1.03×10^{-5}	9.76×10^{-5}	1.43×10^{-4}	1.22×10^{-4}	0.122
15d	1.07×10^{-5}	9.80×10^{-5}	9.86×10^{-5}	1.07×10^{-4}	0.116
15a	1.10×10^{-5}	1.07×10^{-4}	1.40×10^{-4}	1.37×10^{-4}	0.121
Mean	1.05×10^{-5}	1.01×10^{-4}	1.32×10^{-4}	1.20×10^{-4}	0.120
RE	4.67%	1.01%	31.77%	20.17%	10.79%

The comparison of the predicted results from SA and EKF demonstrates that SA may not be able to handle the parameter estimation problem properly for the slug test with positive skin effect. In contrast, the EKF which accounts for the uncertainties of measurements in its algorithm gives accurate parameter estimates in these cases. Moreover, the results of EKF approach are not significantly affected by the parameter correlations. The slightly inaccurate estimates of parameters are due to the fact that the parameters are insensitive to the WWL or the relatively small value of k_1. Finally, the computing time using EKF in all scenarios are less than 30 s in a personal computer with 3.6 G Pentium IV CPU and 1 GB RAM while the SA needs 3.6 h and 7.6 h to obtain the optimal parameters when analyzing 20 and 47 WWL data, respectively. In these scenarios, the EKF saves at least 99.8% computing time when comparing with those of the SA.

4 Conclusions

This study aims at investigating the problem of inaccuracy in the skin thickness d_{sk} and aquifer conductivity k_2 estimates for the positive skin scenarios given in Yeh and Chen (2007). The correlation analysis is used to quantify the strength of relationship between normalized sensitivities of WWL with respect to skin and aquifer parameters over 15- and 1,000-second periods. Moreover, the sensitivity analysis is employed to explore the problem of inaccuracy in the parameter k_2 determination. An approach of

Table 6 The target values and predicted results for the same scenario as Table 2c while the analyzed WWL data lasts 180 s (Yeh and Chen 2007, Scenario 10)

| Case | Estimated Results | | | | |
	k_1 (m/s)	k_2 (m/s)	S_{s1} (1/m)	S_{s2} (1/m)	d_{sk} (m)
Target value	1.00×10^{-5}	1.00×10^{-4}	1.00×10^{-4}	1.00×10^{-4}	0.3085
Simulated Annealing					
10a	1.51×10^{-5}	1.01×10^{-4}	3.22×10^{-5}	1.95×10^{-5}	0.756
10b	1.33×10^{-5}	1.00×10^{-4}	4.69×10^{-5}	6.72×10^{-5}	0.588
10c	9.99×10^{-6}	9.93×10^{-5}	9.57×10^{-5}	4.30×10^{-6}	0.243
10d	1.63×10^{-5}	1.05×10^{-4}	2.64×10^{-5}	1.50×10^{-5}	0.940
10e	1.63×10^{-5}	9.62×10^{-5}	2.70×10^{-5}	9.86×10^{-5}	1.104
Mean	1.42×10^{-5}	1.00×10^{-4}	4.56×10^{-5}	4.09×10^{-5}	0.726
RE	41.98%	0.30%	−54.36%	−59.08%	**135.40%**
Extended Kalman Filter					
10a	9.82×10^{-6}	1.06×10^{-4}	1.20×10^{-4}	1.59×10^{-4}	0.312
10b	9.75×10^{-6}	1.07×10^{-4}	1.18×10^{-4}	1.62×10^{-4}	0.308
10c	9.72×10^{-6}	1.05×10^{-4}	1.24×10^{-4}	1.63×10^{-4}	0.306
10d	1.00×10^{-5}	1.09×10^{-4}	1.19×10^{-4}	1.58×10^{-4}	0.329
10e	9.81×10^{-6}	1.05×10^{-4}	1.17×10^{-4}	1.64×10^{-4}	0.311
Mean	9.82×10^{-6}	1.06×10^{-4}	1.20×10^{-4}	1.61×10^{-4}	0.313
RE	−1.75%	6.22%	19.59%	61.25%	1.53%

coupling the EKF with Moench and Hsieh solution (1985) is developed to determine five parameters, k_1, k_2, S_{s1}, S_{s2}, and d_{sk}, in six positive skin scenarios where the k_2 and d_{sk} were not accurately determined in Yeh and Chen (2007).

The results of correlation analysis demonstrate that the normalized sensitivity to parameter d_{sk} correlates negatively with other parameters. Those high correction values indicate that the parameters k_1 and d_{sk} may be difficult to accurately determine by SA shown in Yeh and Chen (2007). In addition, the results of sensitivity analysis show that the normalized sensitivities of WWL with respect to aquifer parameters (k_2 and S_{s2}) decrease significantly if the skin conductivity k_1 is relatively small, say, 10^{-6} m/s, in the positive skin scenario. Consequently, the aquifer hydraulic properties can not respond to the test quickly and influence the WWL data. This may be the reason why the parameter k_2 was accurately determined in Yeh and Chen (2007, Scenario 14).

Tables 2, 3, 4, 5, 6 and 7 display the predicted results for six positive skin scenarios analyzed by both SA and EKF. The results indicate that the EKF provides much better estimates on parameters k_2 and d_{sk} even the skin thickness is thin. Such results are attributed to the fact that the EKF accounts for the uncertainties of the measurement (round-off errors in WWL data set) in the algorithm. The predicted parameter S_{s2} using EKF is slightly inaccurate since it is very insensitive in response to the measurement error in WWL data. Moreover, the results listed in Table 7 using EKF show that the aquifer parameters k_2 and d_{sk} are difficult to accurately determine when the skin conductivity k_1 is very small because the small value of k_1 retards the propagation of the change of WWL from the test well to the aquifer. The comparison

Table 7 The target values and predicted results for a positive skin aquifer with a distinct difference in the hydraulic conductivities of skin and formation zones (Yeh and Chen 2007, Scenario 14)

| Case | Estimated Results | | | | |
	k_1 (m/s)	k_2 (m/s)	S_{s1} (1/m)	S_{s2} (1/m)	d_{sk} (m)
Target value	1.00×10^{-6}	1.00×10^{-4}	1.00×10^{-4}	1.00×10^{-4}	0.3085
	Simulated Annealing				
14a	1.00×10^{-6}	8.51×10^{-4}	9.70×10^{-5}	8.51×10^{-6}	0.315
14b	1.00×10^{-6}	6.51×10^{-4}	9.41×10^{-5}	8.97×10^{-5}	0.315
14c	1.03×10^{-6}	6.59×10^{-4}	9.94×10^{-5}	5.50×10^{-5}	0.349
14d	1.38×10^{-6}	8.33×10^{-5}	4.87×10^{-5}	7.10×10^{-5}	0.623
14e	1.02×10^{-6}	7.66×10^{-4}	9.97×10^{-5}	9.11×10^{-5}	0.324
Mean	1.09×10^{-6}	6.02×10^{-4}	8.78×10^{-5}	6.31×10^{-5}	0.385
RE	8.60%	**502.06%**	−12.22%	−36.94%	24.86%
	Extended Kalman Filter				
14a	1.00×10^{-6}	1.51×10^{-4}	9.74×10^{-5}	1.50×10^{-5}	0.311
14b	9.90×10^{-7}	1.51×10^{-4}	9.70×10^{-5}	1.50×10^{-5}	0.306
14c	9.84×10^{-7}	1.51×10^{-4}	1.10×10^{-4}	1.50×10^{-5}	0.317
14d	1.03×10^{-6}	1.48×10^{-4}	9.68×10^{-5}	1.50×10^{-5}	0.324
14e	9.92×10^{-7}	1.53×10^{-4}	1.06×10^{-4}	1.50×10^{-5}	0.304
Mean	9.99×10^{-7}	1.51×10^{-4}	1.01×10^{-4}	1.50×10^{-5}	0.312
RE	−0.13%	50.88%	1.46%	50.12%	1.25%

of the computing time required by the EKF and the SA also indicates that the EKF is more efficient than the SA in parameter determination.

References

Butler JJ Jr (1998) The design, performance, and analysis of slug tests. Lewis Publishers, Boca Raton, p 252

Bouwer H, Rice RC (1976) A slug test method for determining hydraulic conductivity of unconfined aquifers with completely or partially penetrating wells. Water Resour Res 12(3):423–428

Chen JS, Liu CW, Chen CS, Yeh HD (1996) A Laplace transform solution for tracer tests in a radially convergent flow field with upstream dispersion. J Hydro 183:263–275

Chou C (2011) A threshold based wavelet denoising method for hydrological data modelling. Water Resour Manag 25(7):1809–1830

Cooper HH, Bredehoeft JD, Papadopulos IS (1967) Response of a finite-diameter well to an instantaneous charge of water. Water Resour Res 3(1):263–269

Crump KS (1976) Numerical inversion of Laplace transforms using a Fourier series approximation. J Assoc Comput Mach 23(1):89–96

de Hoog FR, Knight JH, Stokes AN (1982) An improved method for numerical inversion of Laplace transforms. Society for Industrial and Applied Mathematics. J Sci Stat Comput 3(3):357–66

Drécourt JP (2003) Kalman filtering in hydrological modeling, DAIHM Technical Report 2003–1. DHI Water and Environment, Agern, Hørsholm, Denmark

Faust CR, Mercer JW (1984) Evaluation of slug tests in wells containing a finite-thickness skin. Water Resour Res 20(4):504–506

Goegebeur M, Pauwels VRN (2007) Improvement of the PEST parameter estimation algorithm through extended Kalman filtering. J Hydro 337(3–4):436–451

Grewal MS, Andrews AP (1993) Kalman Filtering: Theory and Practice. Prentice Hall, New Jersey

Huang YC, Yeh HD (2007) The use of sensitivity analysis in on-line aquifer parameter estimation. J Hydro 335(3–4):406–418

Hvorslev MJ (1951) Time lag and soil permeability in ground-water observations. Bull. No. 36, Waterways Exper Sta, Corps of Engrs, Vicksburg, Miss

Hyder Z, Butler JJ Jr, McElwee CD, Liu WZ (1994) Slug tests in partially penetrating wells. Water Resour Res 30(11):2945–2957

IMSL (2003) MATH/Library, vol 1. Visual Numerics, Houston TX

Lee W, Lee K, Kim SU, Chung ES (2010) The development of rating curve considering variance function using pseudo-likelihood estimation method. Water Resour Manag 24(2):321–348

Leng CH, Yeh HD (2003) Aquifer parameter identification using the extended Kalman filter. Water Resour Res 39(3):1062. doi:10.1029/2001WR000840

McLaughlin D, Townley LR (1996) A reassessment of the groundwater inverse problem. Water Resour Res 32(5):1131–1161

Moench AF, Hsieh PA (1985) Analysis of slug test data in a well with finite-thickness skin. In Memoirs of the 17th international congress on the hydrogeology of rocks of low permeability. 17:17–29, U.S.A. Members of the International Association of Hydrogeologists, Tucson, Ariz

Nenna V, Pidlisecky A, Knight R (2011) Application of an extended Kalman filter approach to inversion of time-lapse electrical resistivity imaging data for monitoring recharge. Water Resour Res 47:W10525. doi:10.1029/2010WR010120

Ramey HJ Jr, Agarwal RG, Martin I (1975) Analysis of "Slug Test" or DST flow period data. J Can Pet Technol 14(3):37–47

Rani D, Moreira M (2010) Simulation–optimization modeling: A survey and potential application in reservoir systems operation. Water Resour Manag 24(6):1107–1138

Shamir E, Lee BJ, Bae DH, Georgakakos KP (2010) Flood forecasting in regulated basins using the Ensemble Extended Kalman Filter with the storage function method. J Hydro Eng 15(12):1030–1044

Springer RK, Gelhar LW (1991) Characterization of large-scale aquifer heterogeneity in glacial outwash by analysis of slug tests with oscillatory response. Cape Cod, Massachusetts. US Geol Surv Water Res Invest Rep 91–4034:36–40

Yang SY, Yeh HD (2002) Solution for flow rates across the wellbore in a two-zone confined aquifer. J Hydraul Eng 128(2):175–183

Yeh HD (1987) Theis' solution by nonlinear least-squares and finite-difference Newton's method. Ground Water 25(6):710–715

Yeh HD, Huang YC (2005) Parameter estimation for leaky aquifers using the extended Kalman filter, and considering model and data measurement uncertainties. J Hydro 302(1–4):28–45

Yeh HD, Yang SY (2006) A novel analytical solution for a slug test conducted in a well with a finite-thickness skin. Adv Water Resour 29:1479–1489

Yeh HD, Chen YJ (2007) Determination of skin and aquifer parameters for a slug test with wellbore-skin effect. J Hydro 342(3–4):283–294